Forest dynamics and the growth decline of red spruce and sugar maple on Bolton Mountain, Vermont: a comparison of modeling methods

Daniel G. Gavin, Brian Beckage, and Benjamin Osborne

Abstract: Montane forests in the northeastern United States have experienced symptoms of declining vigor, such as branch dieback and increased mortality, over the last half-century. These declines have been attributed to the cumulative impacts of acid deposition, but reconstructing these declines from tree-ring records has proved difficult because of confounding factors that affect low-frequency growth patterns, including climate and natural growth trajectories following disturbance. We obtained tree-ring records of red spruce (*Picea rubens* Sarg.) and sugar maple (*Acer saccharum* L.) from three elevations on Bolton Mountain, Vermont, and applied traditional dendroclimatological analyses that revealed a profound declining growth–climate correlation since ca. 1970 for sugar maple but much less so for red spruce. We then applied a new multifaceted statistical approach that conservatively detrends tree-ring records by minimizing the influences of tree size, age, and canopy disturbances on radial growth. In contrast with the traditional analysis, this approach yielded chronologies that were consistently correlated with climate but with important exceptions. Low-elevation sugar maple suffered distinct episodes of slow growth, likely because of insect defoliators, and also a progressive decline since ca. 1988. Red spruce experienced subdecadal episodes of decline that may be related to freeze–thaw events known to injure foliage but showed no evidence of a progressive decline. This analysis was supported by a forest plot resurvey that indicated major declines in these species.

Résumé : Au cours des 50 dernières années, les forêts alpestres du nord-est des États-Unis ont montré des symptômes de perte de vigueur qui se manifeste par la mort en cime et l'augmentation de la mortalité. Ces dépérissements ont été attribués aux impacts cumulatifs des dépôts acides mais il s'est avéré difficile de les reconstituer à partir des données dendrochronologiques à cause des variables confusionnelles qui affectent les modèles de croissance à basse fréquence, incluant le climat et les trajectoires naturelles de croissance à la suite d'une perturbation. Nous avons obtenus des données dendrochronologiques pour l'épinette rouge (*Picea rubens* Sarg.) et l'érable à sucre (*Acer saccharum* L.) à trois altitudes sur le mont Bolton, au Vermont. Nous avons soumis ces données à des analyses dendroclimatologiques traditionnelles qui ont révélé une forte corrélation entre le climat et la diminution de croissance depuis environ 1970 chez l'érable, mais cette relation était beaucoup moins évidente chez l'épinette. Nous avons ensuite utilisé une approche statistique multi-facettes qui modifie de façon conservatrice les données dendrochronologiques en minimisant l'influence de la dimension et de l'âge des arbres ainsi que celle des perturbations de la canopée sur la croissance radiale. Contrairement à l'analyse traditionnelle, cette approche a produit des chronologies constamment corrélées avec le climat mais avec d'importantes exceptions. L'érable à sucre situé à faible altitude a connu des épisodes distincts de croissance réduite, probablement à cause des insectes défoliateurs, ainsi qu'un dépérissement progressif depuis environ 1988. L'épinette rouge a connu des épisodes de dépérissement qui ont duré moins de 10 ans et qui pourraient être reliés à des cycles de gel-dégel qui causent des dommages au feuillage mais cette espèce n'a pas montré de signes de dépérissement progressif. Cette analyse est supportée par un nouveau mesurage de places-échantillons forestières qui a révélé que ces espèces subissaient un dépérissement majeur.

[Traduit par la Rédaction]

Introduction

The detection of decadal-scale growth declines of sugar maple (*Acer saccharum* L.) and red spruce (*Picea rubens* Sarg.) in the northeastern United States has been plagued by the difficulty of disentangling multiple factors that operate at both high and low frequencies (Cook and Zedaker 1992; Horsley et al. 2002). These species have been physiologically impacted by acid deposition via well-understood mechanisms (St. Clair et al. 2008). Acid deposition indirectly limits nutrient availability through leaching of soil calcium and mobilization of aluminum, which then reduce tree nutrition (Schaberg et al. 2001). This may lead to reduced leaf area, total photosynthetic carbon capture, and defensive mechanisms, which in turn predispose trees to additional stresses such as defoliation and winter injury (e.g., Horsley et al. 2002). Eventually susceptibility to secondary pathogens furthers the growth decline and leads to visible dieback and

Received 24 February 2008. Accepted 25 June 2008. Published on the NRC Research Press Web site at cjfr.nrc.ca on 12 September 2008.

D.G. Gavin,[1,2] B. Beckage, and B. Osborne. Department of Plant Biology, University of Vermont, Burlington, VT 05405-0086, USA.

[1]Corresponding author (e-mail: dgavin@uoregon.edu).
[2]Present address: Department of Geography, 1251 University of Oregon, Eugene, OR 97403-1251, USA.

 doi:10.1139/X08-106

death (Manion 1991). In addition to defoliation and freezing events, growth trends may be affected by other more slowly varying factors that interact with acid deposition, including nitrogen deposition (McLauchlan et al. 2007) and climate change (Hamburg and Cogbill 1988).

Tree-ring records are a logical means of reconstructing the progression of decline conditions, but with respect to red spruce and sugar maple, the conclusions regarding the existence of growth declines has depended upon the statistical approach employed (Cook and Zedaker 1992). Standard dendroclimatological methods detrend the time series of ring widths from individual cores preserving high-frequency variation but removing much of the low-frequency variation (Cook et al. 1995). These methods have revealed a shifting growth–climate relationship during the 1960s, which is consistent with the introduction of additional impacts from acid deposition (Johnson et al. 1988). Examination of nondetrended tree-ring records, in contrast, has supported a stand-dynamics explanation; disturbances prior to the 1960s initiated a trajectory of growth release followed by increased competition for canopy space during the 1960s (Cook 1990; Reams and Van Deusen 1993), although this interpretation remains debated (LeBlanc 1992; Johnson et al. 1995). Although few tree-ring studies have addressed sugar maple decline, there is a similar dichotomy related to analytical method (Payette et al. 1996; Duchesne et al. 2002). Thus, (*i*) the amount of low-frequency variation in growth that may be explained by stand dynamics and (*ii*) whether growth declines are composed of discrete episodes from which trees recover or whether they represent a persistent reduction in vigor resulting from multiple causal agents remains unclear from tree-ring studies (Cherubini et al. 1998).

An alternative approach to detrending tree-ring records is regional-curve standardization (RCS; Briffa et al. 1992). RCS has received renewed attention because of its potential to preserve more low-frequency variation than possible using standard detrending methods (e.g., Esper et al. 2002). This method involves developing a single curve to describe the regional age-related growth trend and then uses this curve to detrend individual growth records (Briffa et al. 1992). Although RCS has been successfully applied to open-grown trees where an age-related pattern may be clearly detected (Esper et al. 2002), RCS is more difficult to use in closed-canopy forests in which canopy disturbances greatly affect the light environment and overprint any age-related growth trend (Esper et al. 2003). More recent developments, however, have extended the method to include both age and size effects on growth, potentially increasing its applicability to closed forests (Melvin 2004).

The goal of this study is to reconstruct the low-frequency growth chronology of sugar maple and red spruce, in order to distinguish the effects of natural stand dynamics, disturbance, and climate. To do this, we first used a standard dendroclimatological approach to determine the correlation between the high-frequency variation in growth and a set of predictive climate variables. We then present a multifaceted approach to decomposing tree-ring records from mesic forests that preserves both low- and high-frequency variation in growth. This method is intended to minimize the effects of, in order, (*i*) the "biological growth trend" related to tree age and size, (*ii*) the effect of canopy disturbances through the comparison of subcanopy and canopy trees, and (*iii*) the role of climate as predicted by a time-series model. Any unexplained growth pattern following these steps may be the result of discrete disturbances or declining tree vigor. We apply these methods to new records from three elevations on Bolton Mountain, Vermont: the middle and upper elevation ranges of sugar maple in northern hardwoods forest (550 and 725 m a.s.l.) and the lower and middle elevation ranges of red spruce in subalpine conifer forest (725 and 900 m a.s.l.). Finally, we use forest surveys at our study sites from 1964 and 2004 to assess whether growth declines identified in tree cores corresponded to stand-wide demographic trends.

Materials and methods

Rationale for detrending tree-ring data

The RCS method estimates the regional age-dependent growth response that is independent of time (year) and applies this single standardization curve to all cores. Therefore, it is necessary that the growth data used to calibrate an RCS curve come from trees that span a wide range of establishment dates. In our application of this method to shade-tolerant trees in closed-canopy humid forests, growth suppression and release events may overprint any age-related trend. Similar to methods proposed by Melvin (2004), we extend the RCS method to include past tree size and its interaction with age as predictors of ring width; small old trees would be expected to grow more slowly than large young trees. To apply this approach, we selected trees across a wide range of sizes and ages to obtain a data set in which (*i*) the mean age and size of trees does not change dramatically over time and (*ii*) there is no sampling bias towards the largest trees that may be experiencing natural senescence (Cherubini et al. 1998). Whereas RCS detrending is typically applied to long tree-ring records from live and dead trees (Esper et al. 2003), our application is to records from only live and relatively young trees. Nevertheless, we are interested in preserving frequencies of variability of only 40–80 years that would be compromised by traditional detrending methods (i.e., core-by-core curve fitting).

Removing the age- and size-related growth trends is unlikely to remove the effects of canopy disturbance and associated growth releases. We identified periods of widespread canopy disturbance and associated growth releases by examining the growth patterns of trees in size bands (i.e., the mean growth for trees within a certain size class during each year) that represent canopy or subcanopy trees. Our rationale is that canopy disturbances (i.e., mortality of neighbouring trees) that create light gaps result in a greater growth responses for trees of intermediate and suppressed crown sizes compared with large trees with exposed crowns. Small size bands should reflect subcanopy growth rates, whereas large size bands should reflect growth rates of trees with greater crown illumination and thus with less capacity to experience growth releases (Black and Abrams 2004). A large increase in growth in small-size bands compared with larger-size bands is indicative of a canopy release event, and censoring the smaller-diameter band should greatly reduce the effects of canopy disturbances. LaMarche (1974) used a similar censoring of the innermost tree rings.

Table 1. Sample sizes of each species at each elevation at Bolton Mountain, Vermont.

Elevation (m a.s.l.)	Species	No. of trees	No. of cores	No. of trees aged	Mean pith dates*
550	Sugar maple	60	182	55	1906 (1770–1950)
725	Sugar maple	46	133	43	1904 (1849–1956)
725	Red spruce	52	102	45	1860 (1653–1942)
900	Red spruce	38	76	38	1883 (1664–1957)

*Values in parentheses are the ranges of dates.

These analyses result in a minimally detrended chronology that preserves low frequency variation and leaves temporal structure in the chronology. We are left with the challenge of modeling the effect of climate on growth rates on a mean tree-ring chronology that contains a high level of autocorrelation. We use an autoregressive (AR) time-series model in which growth each year is a function of growth in the previous 1 or 2 years (AR1 and AR2, respectively) in addition to one or more independent climate variables (Fritts and Guiot 1990). In contrast, complete removal of the autocorrelation structure prior to comparison with climate data removes the low-frequency variability that we wish to assess. We calibrate and verify the model prior to the onset of the hypothesized anthropogenic impacts such as acid deposition and then assess the degree to which more recent growth diverges from that predicted (Johnson et al. 1988). Finally, we also evaluated the growth–climate relationship using standard methods of detrending that preserve the high-frequency component of growth. Comparison of these methods reveals their relative merits and provides further evaluation of climate and stand dynamics on growth trends.

Study area

We sampled forests on the west-facing slope of Bolton Mountain, Vermont (42°27′N, 72°51′W), during summer 2005. The forest comprises mainly sugar maple, yellow birch (*Betula alleghaniensis* Britt.), and American beech (*Fagus grandifolia* Ehrh.) at <700 m a.s.l., transitions to red spruce, balsam fir (*Abies balsamea* (L.) Mill.), and mountain paper birch (*Betula cordifolia* Regel) between 700 and 850 m a.s.l., and is dominated by balsam fir with minor amounts of red spruce and mountain paper birch >850 m a.s.l. The area has been minimally impacted by logging disturbances, with evidence for partial logging at lower elevations (<600 m a.s.l.) before the 1950s (Siccama 1974). Soil pits analyzed within the study area revealed a pH of 3.6–4.5 in the rooting zone, which ranged from 15 to 55 cm in depth. Exchangeable calcium concentration, obtained using ammonium nitrate extractant and measured with an inductively coupled plasma-atomic emission spectrometer, decreased from approximately 200 m/kg at 550 m a.s.l. to approximately 25 m/kg at 900 m a.s.l. (Berkman 2006). These values place Bolton Mountain well within the range of forest types that are susceptible to decline symptoms and lower growth due to calcium depletion via acid deposition (Schaberg et al. 2006). However, we noted little evidence of branch dieback, overall canopy thinning, or standing dead trees for either species in 2005.

Fieldwork and core processing

We used sampling points spaced 50 m apart along 2 km transects following the elevational contour, to minimize the signal from patchy asynchronous canopy disturbances. Sampling was stratified in 10 cm diameter classes between 15 and 65 cm. We selected the nearest tree to each sampling point, randomly alternating among size classes along each transect. Red spruce was cored twice parallel to the contour 1.3 m above the ground. Sugar maple was cored three times equidistant around the bole because of the greater potential for missing tree rings in this species (Lorimer et al. 1999). Cores were processed following standard procedures, including crossdating to ensure calendar-year assignments to annual tree rings. Ring widths (i.e., radial growth) were measured using a sliding-scale micrometer. Total sample sizes are shown in Table 1.

Statistical methods

We first constructed chronologies that emphasize high-frequency variation using standard detrending methods in ARSTAN 4.1 software (Cook 1985). Ring widths were power-transformed using a method that corrects for the correlation between the mean and variance in each core (Cook and Peters 1997). Each power-transformed series (from each crossdated core) was fitted with a 49 year smoothing spline, and tree-ring indices were calculated as the difference from the fitted curve. More commonly used methods involve no power transformation but a ratio rather than difference is applied to the fitted curve. However, in many of our cores the fitted curve fell below 0.5 mm, the "danger zone" in which ratios become overly sensitive to the level of the fitted curve (Cook and Peters 1997). Statistically significant autocorrelation of the tree-ring indices (lags up to 2 years) was identified and removed using an autoregressive model. For each species and site, the standardized series were combined using a robust Tukey-biweight mean to produce the "residual" chronology.

We next calculated RCS-detrended chronologies using custom algorithms. The fitting of RCS models first required calculating the ages of each tree and reconstructing past diameter for each year of each tree (hereinafter referred to as "ring diameter"). For all cores that did not intersect the pith, the distance to the pith was estimated by measuring the curvature of the innermost tree ring (Duncan 1989). The number of missing years to the pith was estimated from the width of the innermost tree ring and the distance to the pith. Trees were rejected if this estimate was >15 years for all cores, which reduced our samples by up to eight trees per site. Ring diameters were reconstructed using the pith-to-ring distance in each increment core and assuming that growth occurs proportionally around the bole to calculate past basal area (Bakker 2005). Ring diameters were then calculated from the mean of the basal-area estimates from indi-

vidual cores from each tree. Ring widths were averaged for the period in common between cores from each tree. For sugar maple, we used only the two of three cores that most closely reached the pith.

We developed species-specific RCS models from locally weighted (loess) regressions that predict ring width from ring age, ring diameter, and their interaction. These regressions were fit to ring widths from all years and all trees within each species, resulting in large sample sizes (n = 7522 and 8170 for sugar maple and red spruce, respectively). For fitting the loess model, we used a window that spans 75% of the data so that local estimates of ring widths from the model are not sensitive to short-term growth patterns in individual trees. We used a log-transformation of ring age because young trees often experience rapid changes in their growth environment.

Growth indices were calculated as the ratio of the measured to RCS-predicted values. This ratio method yielded virtually identical time series compared with that obtained by applying the RCS method to power-transformed ring widths and using differences because the RCS model did not fall below the 0.5 m danger zone (Cook and Peters 1997). Therefore, we chose to use ratios because they have the advantage that growth may be expressed as a percentage of the RCS-predicted value. We calculated mean indices only for years with $n \geq 5$ trees using a robust Tukey-biweight mean.

We examined stand-wide disturbances in two ways. First, sudden growth releases were identified for years when mean ring width during the subsequent 10 years were more than twice that of the previous 10 years (Lorimer and Frelich 1989). Second, we compared growth indices computed for three "diameter bands" (i.e., size classes based on reconstructed diameter) to determine the mean growth of trees of similar size over time. We noted that the small-size band showed sustained releases following disturbances (which we expected as discussed above), whereas the larger-size bands showed no such trends. We thus censored the <20 cm size band and retained the larger bands in what we call the "size-band" chronology. Confidence intervals for the size-band chronology were calculated using a stratified bootstrap. Bootstrap samples were calculated by resampling trees with replacement using the same stratified sampling of trees in 10 cm diameter classes that was used to select trees in the field. Confidence intervals (95%) were calculated from the distribution of 999 bootstrap samples of the size-band chronology.

Growth–climate correlation

We compared both the residual chronologies and the size-band chronologies with a suite of monthly climatic and bioclimatic variables. Daily precipitation and temperature maxima and minima from Burlington International Airport (20 km west of the study area) for the period 1884–2002 were obtained from the US Historical Climatology Network and extended through 2004 using archived data from the National Climatic Data Center after noting no difference between the two data sets for the period 2000–2002.

The daily climate data were used to directly calculate monthly mean temperature and monthly precipitation and four bioclimatic variables: growing degree-days on a 4 °C base (GDD, previous-year 1 November – 31 October), actual evapotranspiration (April–August), the standardized precipitation index (April–August), and the Palmer drought severity index (PDSI, annual). For the bioclimatic variables, we adjusted the daily observations to the elevation of each of the three sites using a monthly environmental lapse rate based on the temperature difference between Burlington (90 m a.s.l.) and the summit of Mount Mansfield (1330 m a.s.l., 12 km north of Bolton Mountain).[3]

For the residual chronologies, we assessed the climatic controls of growth using the software DENDROCLIM2002 (Biondi and Waikul 2004). This algorithm generates correlation coefficients for each climatic variable as well as the weights of each variable in a response function (Guiot 1993). The first analysis used monthly temperature and precipitation for the months of April of the previous year through August of the current year (32 predictors). The second analysis used only the four bioclimatic variables. The large number of variables in the first analysis may yield spurious correlations; therefore, we present only the results from the more conservative response-surface analysis. Significance of coefficients was calculated using bootstrap resampling with statistical significance reported for $P < 0.05$. These analyses were run for the period 1910–1955 because this predates the hypothesized onset of severe growth declines in red spruce, lacks white rings (narrow tree rings with a likely non-climatic cause, as discussed below), and contains sufficient degrees of freedom for the analyses (Biondi and Waikul 2004). We then examined the time stability of the growth–climate relationship for the most predictive variables by calculating the correlation coefficient in a 21 year moving window over the entire chronology at each site.

For the size-band chronologies, we assessed the climatic controls of growth using autoregressive time-series modeling. We used Akaike's information criterion (AIC) to select the most parsimonious model from a suite of models constructed with one or two autoregressive terms and the same set of climate variables used in the response-function analysis, using 1935–1955 as the calibration period. This calibration period differed from that used by the response-function analysis above because large-size bands were necessarily shorter in length, especially for high-elevation red spruce. To make the model fits comparable, the calibration period needed to be the same among all chronologies. However, for the chronologies in which a longer calibration was possible, the 1935–1955 calibration period produced good fits to the pre-1935 period and models based on a longer calibration period were similar to those based on the 1935–1955 period. To validate the models, we used the correlation coefficient and the reduction of error statistic between observed and pre-

[3] Details regarding calculation of the bioclimatic variables and additional references for standard statistical methods are in the supplementary online material. Supplementary data for this article are available on the journal Web site (cjfr.nrc.ca) or may be purchased from the Depository of Unpublished Data, Document Delivery, CISTI, National Research Council Canada, Building M-55, 1200 Montreal Road, Ottawa, ON K1A 0R6, Canada. DUD 3807. For more information on obtaining material refer to cisti-icist.nrc-cnrc.gc.ca/cms/unpub_e.html.

Fig. 1. Growth–climate response-function coefficients for sugar maple and red spruce. Tree-ring chronologies for each of the four species and site combinations are the ARSTAN (detrended) residual chronologies for the period 1910–1959. Two analyses were run for each chronology: (*i*) monthly temperature and precipitation for the period from May of the previous year to August of the current year (32 predictors) and (*ii*) four bioclimatic variables. GDD, growing degree-days; AET, actual evapotranspiration; SPI, standardized precipitation index; PDSI, Palmer drought severity index. Asterisks indicate variables with a significant correlation with growth at $P < 0.05$.

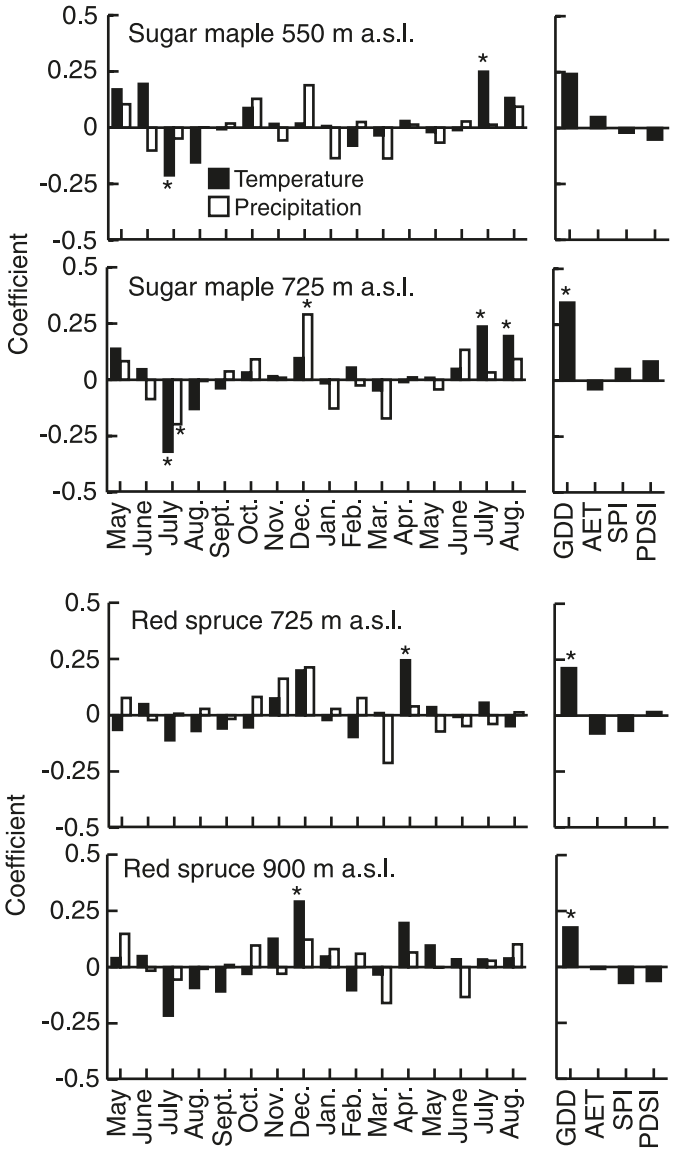

dicted indices calculated in a moving 21 year window. The latter statistic is a measure of the amount of variability explained relative to that explained by only the mean value of the calibration period and is thus sensitive to both the variation and magnitude of the predicted values (Fritts and Guiot 1990). All analyses (except the DENDROCLIM2002 analysis) were calculated using the R statistical language.[4]

Vegetation survey

In 1964, T.G. Siccama (1974) surveyed forest composition along the same elevation gradient on Bolton Mountain where we cored trees. We resurveyed these stands in 2004 using the same methods employed in 1964 (Beckage et al. 2008). Sampling was conducted at 60 m intervals between 549 and 1097 m a.s.l. At each elevation, 5–10 plots 3 m × 30.5 m in area were placed parallel to each other, spaced by 15.2 m, and perpendicular to the contour. The species and diameter of all live trees >2 cm in diameter were recorded. In 2004, the plots were relocated using GPS and altimeter (±3 m) and forests were sampled following the same methods.

Results

Response-function analysis

Several bioclimatic and monthly climatic variables have statistically significant coefficients ($P < 0.05$) in the response-function analyses with each of the residual chronologies, which emphasize the high-frequency component of growth variation (Fig. 1). For sugar maple at both elevations, significantly positive coefficients were found for July temperature in the current year and negative coefficients for July temperature of the previous year. GDD and precipitation have inconsistent coefficients between sites. We selected current-year July temperature for an additional correlation analysis with sugar maple. In a moving 21 year window, the correlation of the sugar maple residual chronology with July temperature decreases rapidly during the mid-1960s, reaching a minimum in the early 1980s, which has not fully recovered (Fig. 2). For red spruce, response-surface analysis shows significant coefficients for GDD (at both elevations), and for April (at 725 m a.s.l.) or December (at 900 m a.s.l.) temperature (Fig. 1). We selected GDD for an additional correlation analysis with red spruce. In a moving 21 year window, the correlation of the red spruce residual chronology with GDD is sporadically significant through the mid-1970s and then declines to nonsignificant levels only at the lower elevation site (725 m a.s.l.; Fig. 2).

RCS models and size-band detrending

RCS models using only ring age or ring diameter were not significant (results not shown), but models including the interaction of these variables explains 16% and 21% of the variation in radial growth in sugar maple and red spruce, respectively (Fig. 3). Site-specific RCS models are very similar among elevations but within species (not shown), so a single RCS model is used for each species. The variation in radial growth explained by the RCS models occurs mainly among trees rather than within trees. Specifically, the amount of variation explained by the RCS model on a per-tree basis is very low, ranging from 3% to 10% for both species. This lack of explained variation is due to persistent differences in growth rates among trees, possibly related to microsite conditions (Landis and Peart 2005). Thus, because individual trees "follow the contour" on the RCS surface (Fig. 3), the main effect of RCS is to standardize individual chronologies based on their absolute growth rates.

[4] Custom algorithms used in this paper are available from geography.uoregon.edu/gavin [accessed 26 August 2008].

Fig. 2. Pearson's correlation between the residual chronologies and July temperature (sugar maple) and GDD (red spruce) in a 21 year moving window. Horizontal lines indicate the years in which the correlation coefficient was significant at $P < 0.05$. Significant correlations were assessed using bootstrap resampling.

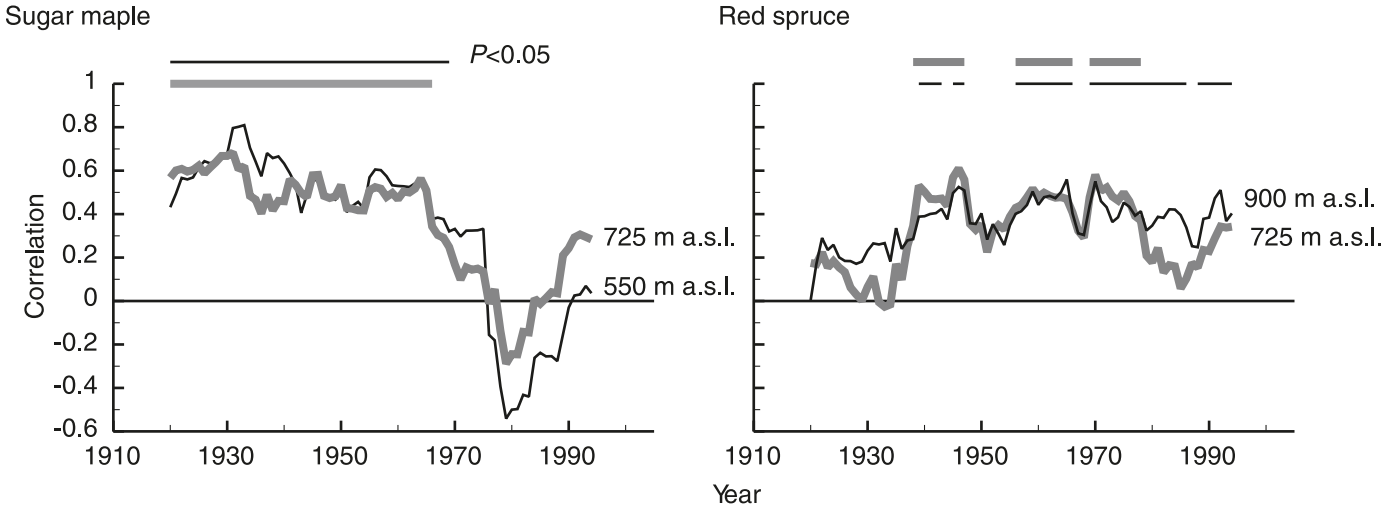

The size-band decomposition identified the impact of disturbances on small trees and resulted in chronologies with little bias due to size and age of trees (Figs. 4 and 5). Specifically, the 5–20 cm size bands of both species show the greatest low-frequency variability suggestive of periods of suppression followed by disturbance-incited growth release, with all of the sudden release events occurring within trees of this size. In contrast, the larger-size bands (>20 cm) have growth trajectories that are largely independent of these disturbances. Within these size bands, the mean age and size of our sampled trees is stationary over time (Figs. 4 and 5). The extended RCS method removed the effects of size and age simultaneously, effectively making distinct RCS curves for trees of different mean growth rates. Thus, a "modern sample bias" that may result when natural mortality censors old fast-growing trees from the RCS curve appears to be of little or no importance in our case (Melvin 2004). The only exception is for sugar maple at 725 m a.s.l., where the mean age in the >35 cm size band increases with time, likely because of a pulse of sugar maple recruitment at this elevation (Beckage et al. 2008). Bias at this site has been minimized by the stationarity of ring diameter over time (Fig. 4).

We recorded several instances of so-called "white rings," that is, sugar maple tree rings in which growth was markedly lower and followed by a very narrow or missing tree ring. In other hardwood species, this phenomenon has been attributed to defoliation of >90% of the canopy by insects (Hogg et al. 2002). For sugar maple, the most likely insects are forest tent caterpillars (*Malacosoma disstria* Hübner, 1820; Cooke and Lorenzetti 2006) and, since the mid-1980s, pear thrips (*Taeniothrips inconsequens* Uzel, 1895; Allen et al. 1992), although we do not preclude severe winter storms as another defoliating mechanism. White rings in sugar maple are common during only 3 years. At the 550 m site, the extremely slow growth during 1965 (<50% of that expected in large trees) is preceded by a white ring in 36% of the trees sampled. White rings at the 550 m site are also common in 1985 (10% of the trees). At the 725 m site, white rings are found in 1964 and 1980 (22% and 17% of the trees, respectively), although growth responses were are muted at the higher elevation.

Climatic controls of radial growth

For each of the four size-band chronologies (i.e., growth only when trees were >20 cm diameter), the most parsimonious model explaining radial growth is a first-order autoregressive model that included the same climate variable identified by the response-function analyses (Table 2).[5] For sugar maple at both elevations, growth is best predicted by July temperature. Sugar maple at its upper elevational limit (725 m a.s.l.) does not show the large multidecadal fluctuations in growth as seen in co-occurring red spruce. Rather, the growth chronology shows high interannual variability that is largely explained by climate (i.e., in the time-series model, there is a high coefficient for July temperature and low coefficient for growth during the previous year; Table 2). The correlations between the model predictions and the observed growth remain high (>0.5) for at least 15 years following the 1935–1955 calibration period. During the 1970s, correlations decline and the reduction of error statistic reaches zero, indicating no additional variation explained relative to the mean of the calibration period. The time-series model predictions generally fall within the confidence intervals of the growth chronologies at both elevations with a few important exceptions (Fig. 6). For example, at 550 m a.s.l., narrow tree rings in 1965, 1988–1989, and several years in the 1990s and 2000s fall below the model predictions.

For red spruce at both elevations, radial growth is best predicted by GDD (Table 2). At 725 m a.s.l., the time-series model assigned more weight to GDD than to the growth of the previous year, but at 900 m a.s.l., the previous year's growth is slightly more important than GDD (Table 2). The model predictions remain correlated with observed values, and the reduction of error statistic remains >0.5 well beyond the 1935–1955 calibration period, despite multidecadal fluctuations in the size-band chronology (Fig. 7). Furthermore,

[5] See Table S1 for a complete comparison of model fits using 40 climate variables.

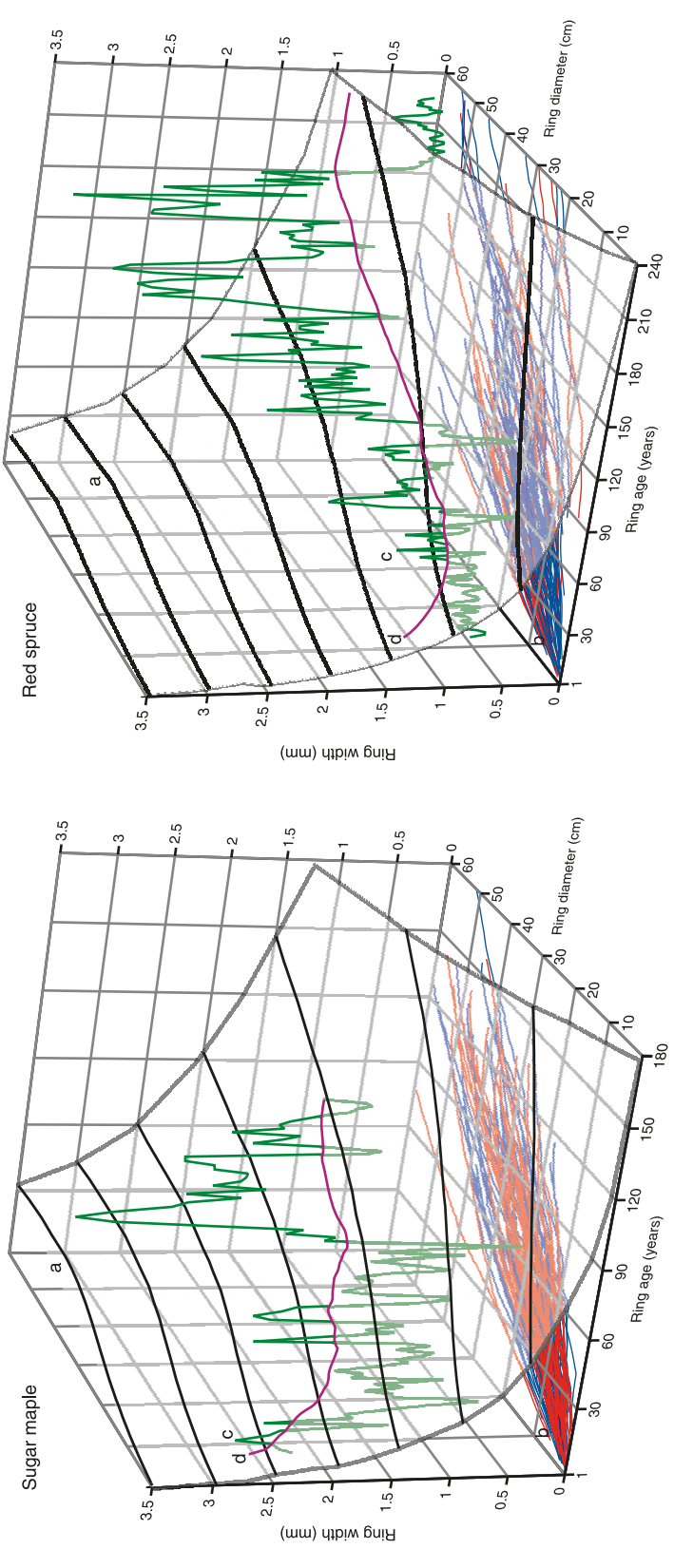

Fig. 3. Response surfaces of ring width as a function of diameter and age for each year (i.e., ring diameter and ring age). Contour lines (line a) show 0.5 mm increments in ring width. Each surface is based on all ring widths (means within trees) measured for each species. "Spaghetti plots" of growth curves (line b), plotted as trajectories of each tree's increasing diameter and age, are shown on the "floor" of each plot. In the Web version, red and blue lines indicate trajectories of trees at the high and low elevation sites, respectively. For each species, an example of one such trajectory is plotted in 3D space moving above and below the response surface (line c). The predicted ring width (i.e., the response–surface value for each year of growth, line d) is used to standardize ring width series from each tree.

Fig. 4. Sugar maple ring widths and growth indices. The top row shows the mean ring width and growth index for all trees at each elevation. Indices were calculated as the ratio of the ring width to predicted values from the response surfaces in Fig. 3. The similarity of the raw ring widths and growth indices reveals the minimal detrending achieved by the RCS curve. Filled curves below show the changing mean ring age, mean ring diameter at breast height (DBH), and sample depth (number of trees). The lower three rows are for three size bands, which are the subset of trees whose ring diameters falls within a range of sizes. Note that the set of trees in each size band changes over time as trees become larger, and also that the mean age and size of trees in the two largest size bands change minimally over time. The histogram below the 5–20 cm size band shows the number of trees experiencing growth releases, a pattern seen only in trees within the small size band. For all curves, only years with a sample of four or more trees are shown.

at both elevations, the model predictions remain within the bootstrapped confidence intervals of the size-band chronology and the chronologies show no long-term decline. However, red spruce at 900 m a.s.l. shows distinct episodes of growth reduction during the 1960s, 1980s, and beginning in 2003.

Vegetation survey

The resurvey of forest vegetation revealed striking differences in red spruce and sugar maple abundance at Bolton Mountain between 1964 and 2004. Red spruce, initially only 12% of the basal area in 1964 at elevations >725 m a.s.l., decreases by an average of 39%. Sugar maple basal area at 550 m a.s.l. decreases by a dramatic 53% (from 90% of the total basal area in 1964). This lost sugar maple was replaced by both American beech and yellow birch (Beckage et al. 2008). In contrast, sugar maple at 725 m a.s.l. increases from trace amounts to 18% of the total basal area.

Discussion

Episodic red spruce injury

Our method of decomposing tree-ring records helps address the factors that may mask growth declines of red spruce. Specifically, the major growth releases and subsequent suppression identified in the 5–20 cm size band are attributable to wind and climatic disturbances, and censoring this diameter band minimizes the effect of these disturbances in the remaining data. Without such censoring, the entire data set would support the hypothesis of Reams and Van Deusen (1993) that stand dynamics were a primary cause of decadal-scale growth trends. However, after censoring, the growth records of red spruce at both elevations do not indicate a long-term growth decline. In fact, the resulting size-band chronology was strongly correlated with GDD on both long and short time scales, indicating that red spruce growth in larger size classes was driven primarily by climate (Fig. 7).

For red spruce at 900 m a.s.l., clusters of sudden growth releases in 1894–1900 and 1949–1953 are likely the result of wind disturbances that are fairly common in conifer forests at this elevation (Fig. 5). Indeed, the ages of co-occurring wind-susceptible balsam fir (not shown) suggest that one or more wind disturbances occurred ca. 1950. For red spruce at 725 m a.s.l., a two-decade period of sustained release was initiated in 1937. This release is coincident with a regionally important spring thaw and refreeze event in March–April 1936 that resulted in widespread mortality of yellow birch, a common tree at this elevation (Bourque et al. 2005), although we did not sample yellow birch to verify this. Concurrent dieback of American beech likely contributed to this release following the arrival of the invading beech scale (*Cryptococcus fagisuga* Lind.) and onset of beech bark disease (Houston et al. 1979). Yellow birch and American beech are absent at 900 m a.s.l., where there was no similar growth release. In addition, co-occurring sugar maple at 725 m a.s.l. did not show similar synchronous growth releases; it is likely that growth of sugar maple at its upper-elevational limit is more limited by climate than by competition.

Although we did not identify a persistent growth decline of red spruce, there are several episodes of reduced growth that cannot be explained either by stand dynamics or by climate. Specifically, at 900 m a.s.l. there were several instances of episodic growth reductions to approximately 40% of growth predicted during 1963–1966, 1981–1986, and 2003–2004 (Fig. 7). Each of these episodes co-occurs with or follows freeze–thaw years, events known to cause winter injury to red spruce foliage (Johnson et al. 1988; Lazarus et al. 2006). At 725 m a.s.l., each of these episodes was less distinct and could be largely explained by growing season temperatures, which is consistent with a frequently observed pattern of increasing winter injury with elevation (Lazarus et al. 2004). Although our records are necessarily composed of trees that survived these events, they nevertheless show that growth following injury may recover to that predicted by climate rather than entering a persistent state of low vigor. Overall, our data are consistent with demographic evidence that high red spruce mortality in the 1960s abated in subsequent decades (Battles et al. 2003).

LeBlanc (1992) examined nondetrended growth of red spruce between New York and Maine on an individual-tree basis and found that the prevalence of growth decline increased after the 1960s. LeBlanc (1992) found that this decline could not be attributable to age, stand density, or trees that experienced a prior release. Our approach is distinct from this because we did not distinguish between trees that did or did not experience prior growth release, but rather focused only on trees of a size that are not expected to have large growth responses to canopy disturbance. While our study does not disagree with LeBlanc (1992) in the occurrence of periods of anomalous low growth (especially at 900 m a.s.l.), it did reveal a large release and suppression event at low elevations that is restricted to small trees. If not censored, this suppression may be incorrectly interpreted (Reams and Van Deusen 1993).

In contrast with the inferences of stand history provided by the size-band chronologies, the residual chronologies provided distinctly different information. The significant correlation of growth with July temperature during the year prior to tree-ring formation (Fig. 1) has been widely reported but

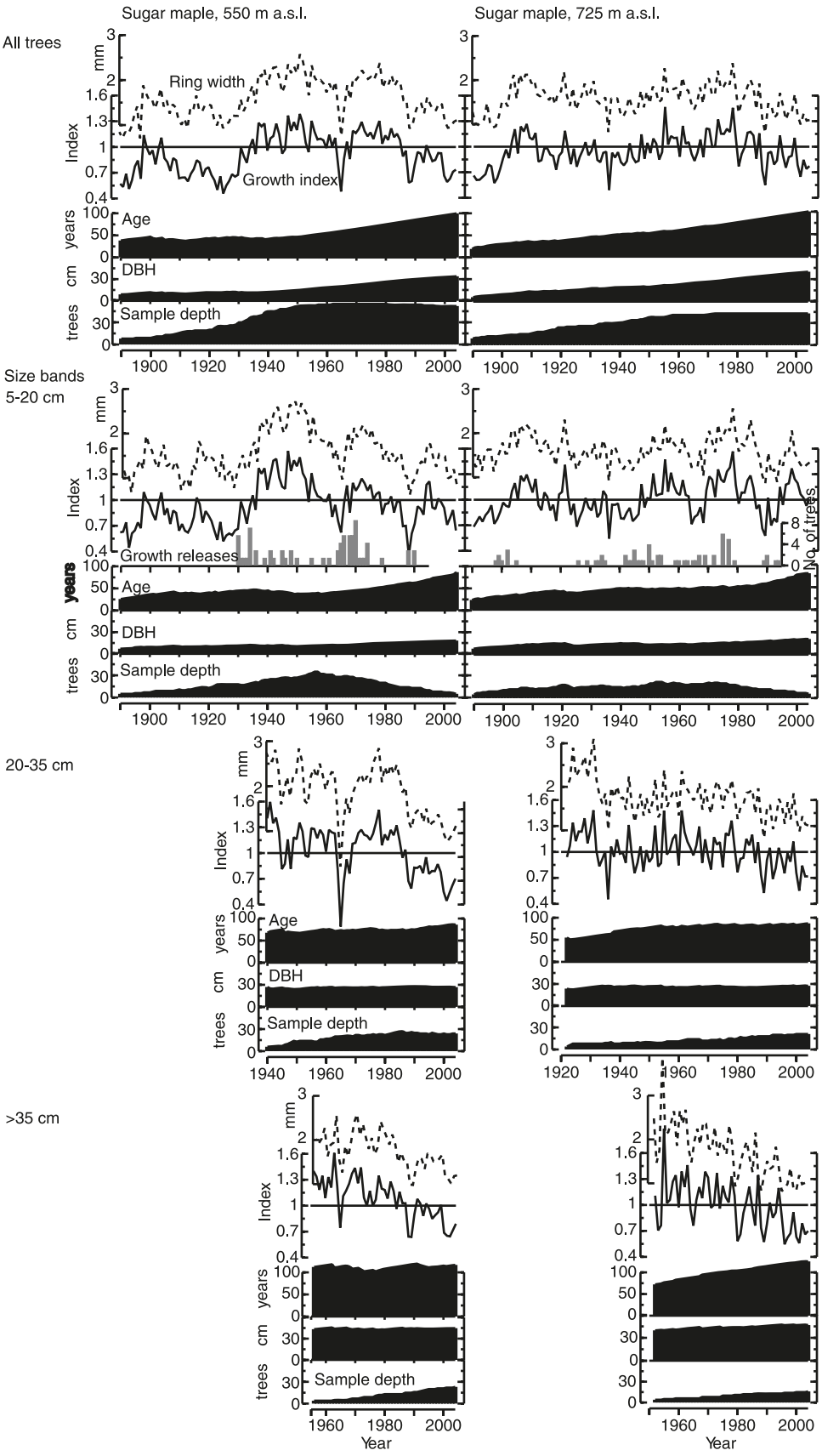

Fig. 5. Red spruce ring widths and growth indices. For an explanation of figure components see Fig. 4.

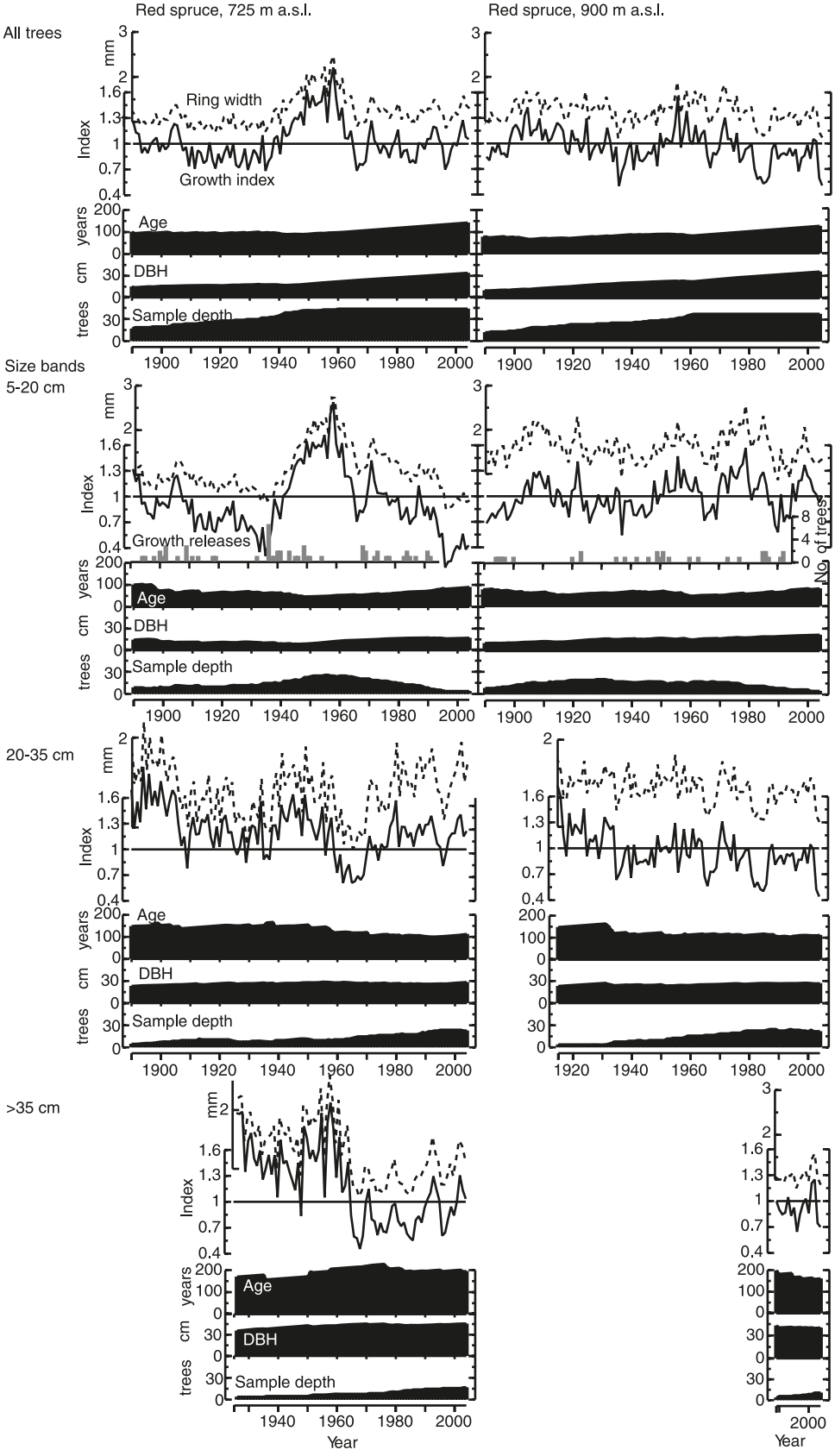

Table 2. Model coefficients and Akaike's information criterion (AIC) values for alternate autoregressive time-series models for predicting radial growth during the 1935–1955 calibration period.

Model coefficients and AIC values	Sugar maple, 550 m a.s.l.	Sugar maple, 725 m a.s.l.	Red spruce, 725 m a.s.l.	Red spruce, 900 m a.s.l.
July temperature	0.579	0.718	0.480	0.452
AR1	0.437	0.138	0.299	0.504
Intercept	0.036	0.007	–0.016	–0.001
AIC	54.9	52.0	59.0	56.9
Growing degree-days	0.162	0.500	0.694	0.609
AR1	0.246	–0.199	0.531	0.682
Intercept	0.035	–0.019	0.005	0.074
AIC	65.6	59.2	48.3	48.9

Note: Models were fit to *z*-scores of all variables. AR1, first-order autocorrelation coefficient. Exploratory analyses using all other climatic variables shown in Fig. 1 yielded poorer fits.

Fig. 6. A model of the growth of sugar maple using an autoregressive time-series model with one independent climate predictor. (A) July temperature in Burlington, Vermont. (B) "Size-band" chronology of sugar maple at 725 m a.s.l. calculated as for the >20 cm size bands in Fig. 4. Background shading indicates 95% bootstrapped confidence intervals of the growth indices. Open triangles show predicted ring widths from a first-order autoregressive time-series model that included July temperature as a predictor. The model was fit for the period 1935–1955 and predicted values plotted for all years. Upward-pointing arrows indicate years with white rings. (C) Model validation statistics calculated in a 21 year moving window. Solid line indicates the Pearson's correlation coefficient and the broken line indicates the reduction of error statistic. (D) and (E) show the same analyses for sugar maple at 550 m a.s.l.

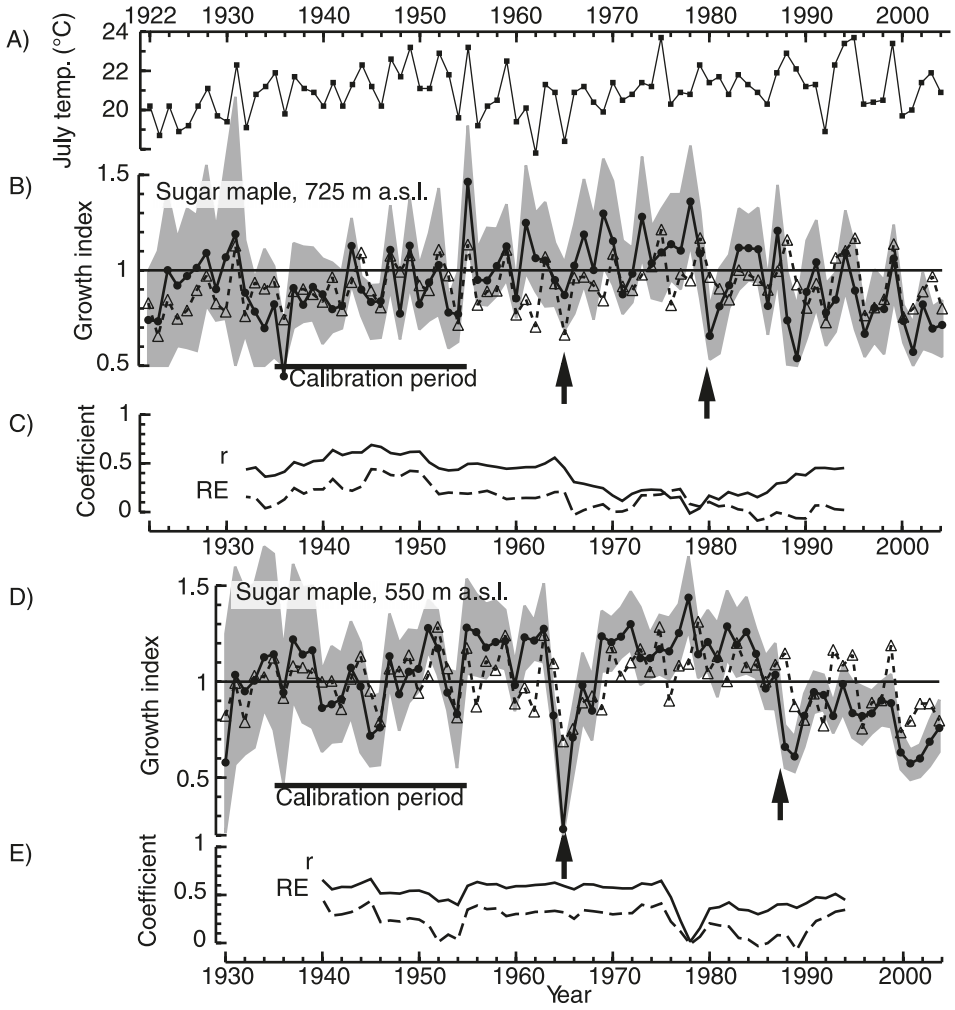

Fig. 7. A model of the growth of red spruce using an autoregressive time series model with one independent climate predictor. For an explanation of figure components see Fig. 6. (A) Annual GDD calculated for 900 m a.s.l. (B) Size-band chronology (solid line) for red spruce. Predicted growth (open triangles) is based on a first-order autoregressive model including GDD as a predictor. (C) Model validation statistics calculated in a 21 year moving window. (D) and (E) show the same analyses for red spruce at 725 m a.s.l.

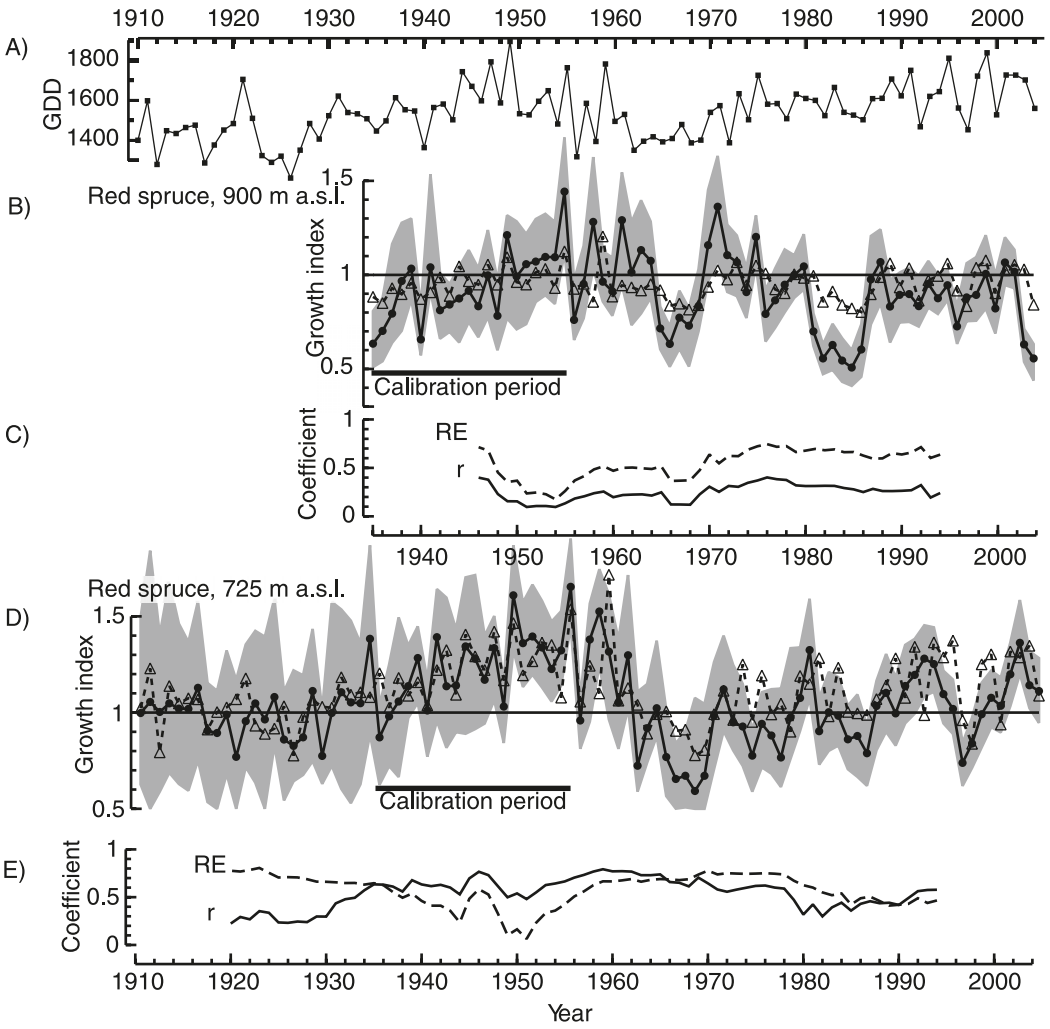

its physiological basis is difficult to explain (Johnson et al. 1988). We chose to focus on GDD because, as a measure of the available energy throughout the year, it is a logical predictor of growth of this evergreen conifer (Schaberg 2000). Interestingly, whereas previous studies have reported a decline in the growth–climate correlation through the 1960s (e.g., Johnson et al. 1988), in this study GDD remained correlated with growth as represented by the size-band chronology (Fig. 7) and, to a lesser degree, the residual chronology (but only at 900 m a.s.l., Fig. 2). These differences may be due to greater predictive capacity of GDD, the variation preserved in the size-band chronology, or to the fact that the sample of trees in 2005 may consist mainly of the most vigorous individuals that were least sensitive to the stressors that caused red spruce mortality episodes of the last several decades. Indeed, the resurvey of the forest composition revealed large decreases in red spruce at 725 and 900 m a.s.l. (Fig. 8). Comparing archived tree-ring data with the data from this study may help address this issue.

Persistent and increasingly severe sugar maple decline

Sugar maple growth history is more complex than that of red spruce, in part because of the impacts of discrete defoliation disturbances. At the 550 m a.s.l. site, growth reductions of increasing duration occurred in 1964–1965, 1986–1989, and from 2000 to present. The presence of white rings and the regional insect outbreak history link the 1964–1965 event to the forest tent caterpillar (Myers 1998; Cooke and Lorenzetti 2006) and the 1986–1989 event to pear thrips (Allen et al. 1992). The most recent event may be connected to the 1998 ice storm, although we note that this storm had no detectable effects on red spruce growth. Whereas growth recovered rapidly following the intense but brief 1964–1965 defoliation, it never fully recovered to expected levels after the 1986–1989 event. Although the trees in these stands showed very little outward appearance of dieback during sampling, our data suggest that this sugar maple population is in a decline that may lead to more severe dieback and mortality in coming years. Duchesne et al. (2002) found that growth declines in sugar maple in southern Quebec often predated visible sign of dieback by one decade.

These results are consistent with other long-term monitoring studies that suggest depletion of soil calcium from acid deposition and episodes of insect outbreaks are resulting in

Fig. 8. Changes in basal area of sugar maple and red spruce from 1964 to 2004 within the study area at Bolton Mountain. Error bars indicate 95% confidence intervals generated from bootstrap resampling of the 5–10 plots at each elevation. Hatched areas indicate the elevations where we collected increment cores. Symbols at each elevation are slightly offset for clarity.

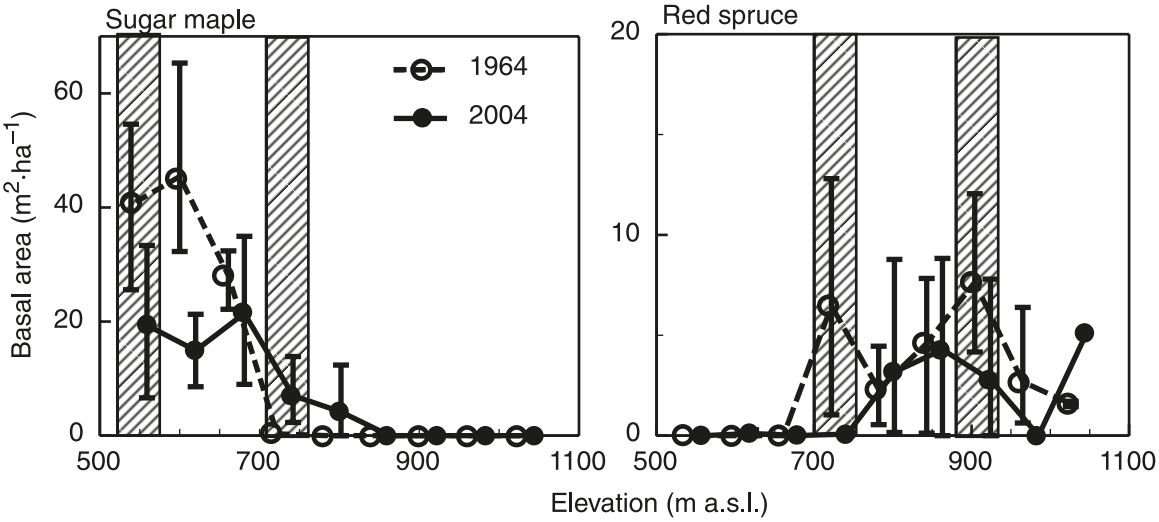

declining sugar maple growth (Horsley et al. 2002). Other processes that may reduce sugar maple include soil freezing due to decreased winter snow cover, shoot-freezing injury during bud break, and ozone exposure, whereas processes that may increase growth include increased atmospheric carbon dioxide and nitrogen availability.[6] These impacts are time varying at many temporal scales, serving to reduce the growth–climate correlation. Several of these factors may be responsible for the decoupling of growth and climate in both the residual chronology (Fig. 2) and the size-band chronology (Fig. 6) through the 1970s.

Two factors may explain elevational differences in the sugar maple records, namely the stronger growth–climate correlation and the less severe growth decline at the higher elevation site (Figs. 2 and 6). First, we found that July temperature is the most important control of sugar maple growth (Fig. 1), in contrast with previous studies that showed a general importance of summer precipitation (Payette et al. 1996; Tardif et al. 2001). Our sites are near or at the upper elevational limits of this species and thus in a cooler and wetter environment than the other studies. The photosynthetic response curve for sugar maple maximizes sharply at 25 °C (Ledig and Korbobo 1983), a daily maximum temperature rarely reached at its elevational limit (725 m a.s.l.). Therefore, increasingly warm summers should greatly improve growth conditions at the high-elevation site, and indeed, growth at 725 m a.s.l. was positively correlated with temperature during the last several decades. Second, tree-ring evidence suggests that the defoliation events were less severe at higher elevations. It is possible that smaller host populations escaped defoliation or colder winters decreased insect survivorship. Together, these factors may have favored sugar maple expansion at higher elevations (Fig. 8).

Conclusions

The slow-growth periods in sugar maple and red spruce at Bolton Mountain were concurrent with widespread mortality, resulting in the loss of basal area at the sites where declines were most severe (low elevation sugar maple and high elevation red spruce; Fig. 8). The striking loss of sugar maple at low elevations is particularly noteworthy and suggests that some regions of Vermont may be experiencing a more severe decline than previously recognized, resulting in changing forest composition (e.g., Hallett et al. 2006). Other sites in the region may not show such a strong sugar maple decline if stands historically experienced mortality of American beech from the invasive beech scale, which may have benefited sugar maple (Lovett and Mitchell 2004). However, at Bolton Mountain, sugar maple did not respond positively to American beech mortality (Beckage et al. 2008) and the sugar maple growth decline may continue for the foreseeable future and produce visible symptoms in the canopy. As shown by the vegetation survey, ingrowth of sugar maple at high elevations may not keep pace with decline at low elevations.

Our approach to tree-ring decomposition has greatly aided the attribution of growth declines with respect to climate and stand-dynamic trajectories. These declines were manifested as discrete injury episodes in red spruce with recovery within a decade or more progressive growth decline following defoliation events of the lower-elevation sugar maple. Taken together, the sugar maple and red spruce tree-ring records and plot resurveys indicate that both short-lived and persistent declines in growth are incited by disturbances and may cause elevational gradients in mortality that ultimately lead to shifting species distributions. At regional scales, however, it is likely that these processes are modified further by substrate type, soil nutrients, and the specific disturbance history (Payette et al. 1996; St. Clair et al. 2008). Additional tree-ring analyses across gradients of disturbance history, soil fertility, and elevation may further elucidate these patterns.

Acknowledgements

We gratefully acknowledge Dan Berkman and Peter Ryan

[6] See supplementary online material for relevant references.

for conducting the soil chemistry study at Bolton Mountain. We also thank Tom Siccama for making the data from the 1964 vegetation plots available and Paul Schaberg and two anonymous referees for comments on the manuscript. This research was supported by the University of Vermont Agricultural Experiment Station federal formula funds, Project VT-H01113, received from the Cooperative State Research, Education and Extension Service, USDA.

References

Allen, D.C., Barnette, C.J., Millers, I., and Lachance, D. 1992. Temporal change (1988–1990) in sugar maple health, and factors associated with crown condition. Can. J. For. Res. **22**: 1776–1784. doi:10.1139/x92-232.

Bakker, J.D. 2005. A new, proportional method for reconstructing historical tree diameters. Can. J. For. Res. **35**: 2515–2520. doi:10.1139/x05-136.

Battles, J.J., Fahey, T.J., Siccama, T.G., and Johnson, A.H. 2003. Community and population dynamics of spruce-fir forests on Whiteface Mountain, New York: recent trends, 1985–2000. Can. J. For. Res. **33**: 54–63. doi:10.1139/x02-150.

Beckage, B., Osborne, B., Gavin, D.G., Pucko, C., Siccama, T.G., and Perkins, T. 2008. A rapid upward shift of a forest ecotone during 40 years of warming in the Green Mountains of Vermont. Proc. Natl. Acad. Sci. U.S.A. **105**: 4197–4202. doi:10.1073/pnas.0708921105. PMID:18334647.

Berkman, D. 2006. An evaluation of soil chemistry for acid deposition on Bolton Mountain, Vermont. B.Sc. thesis. Middlebury College, Middlebury, Vt. Available from www.middlebury.edu/academics/ump/majors/geol/students/theses/2005-2006/dan_berkman.htm. [accessed 1 March 2008].

Biondi, F., and Waikul, K. 2004. DENDROCLIM2002: a C++ program for statistical calibration of climate signals in tree-ring chronologies. Comput. Geosci. **30**: 303–311. doi:10.1016/j.cageo.2003.11.004.

Black, B.A., and Abrams, M.D. 2004. Development and application of boundary-line release criteria. Dendrochronologia, **22**: 31–42. doi:10.1016/j.dendro.2004.09.004.

Bourque, C.P.A., Cox, R.M., Allen, D.J., Arp, P.A., and Meng, F.R. 2005. Spatial extent of winter thaw events in eastern North America: historical weather records in relation to yellow birch decline. Glob. Change Biol. **11**: 1477–1492. doi:10.1111/j.1365-2486.2005.00956.x.

Briffa, K.R., Jones, P.D., Bartholin, T.S., Eckstein, D., Schweingruber, F.H., Karlen, W., Zetterberg, P., and Eronen, M. 1992. Fennoscandian summers from AD-500: temperature changes on short and long timescales. Clim. Dyn. **7**: 111–119. doi:10.1007/BF00211153.

Cherubini, P., Dobbertin, M., and Innes, J.L. 1998. Potential sampling bias in long-term forest growth trends reconstructed from tree rings: a case study from the Italian Alps. For. Ecol. Manage. **109**: 103–118. doi:10.1016/S0378-1127(98)00242-4.

Cook, E.R. 1985. A time series approach to tree-ring standardization, Ph.D. thesis. University of Arizona, Tucson, Ariz.

Cook, E.R. 1990. Bootstrap confidence-intervals for red spruce ring-width chronologies and an assessment of age-related bias in recent growth trends. Can. J. For. Res. **20**: 1326–1331. doi:10.1139/x90-176.

Cook, E.R., and Peters, K. 1997. Calculating unbiased tree-ring indices for the study of climatic and environmental change. Holocene, **7**: 361–370. doi:10.1177/095968369700700314.

Cook, E.R., and Zedaker, S.M. 1992. The dendroecology of red spruce decline. *In* Ecology and decline of red spruce in the eastern United States. *Edited by* C. Eager and M.B. Adams. Springer, New York. pp. 192–234.

Cook, E.R., Briffa, K.R., Meko, D.M., Graybill, D.A., and Funkhouser, G. 1995. The segment length curse in long tree-ring chronology development for paleoclimatic studies. Holocene, **5**: 229–237. doi:10.1177/095968369500500211.

Cooke, B.J., and Lorenzetti, F. 2006. The dynamics of forest tent caterpillar outbreaks in Quebec, Canada. For. Ecol. Manage. **226**: 110–121. doi:10.1016/j.foreco.2006.01.034.

Duchesne, L., Ouimet, R., and Houle, D. 2002. Basal area growth of sugar maple in relation to acid deposition, stand health, and soil nutrients. J. Environ. Qual. **31**: 1676–1683. PMID:12371186.

Duncan, R.P. 1989. An evaluation of errors in tree age estimates based on increment cores in Kahikatea (*Dacrycarpus dacrydioides*). N.Z. Nat. Sci. **16**: 31–37.

Esper, J., Cook, E.R., and Schweingruber, F.H. 2002. Low-frequency signals in long tree-ring chronologies for reconstructing past temperature variability. Science (Washington, D.C.), **295**: 2250–2253. doi:10.1126/science.1066208. PMID:11910106.

Esper, J., Cook, E.R., Krusic, P.J., Peters, K., and Schweingruber, F.H. 2003. Tests of the RCS method for preserving low-frequency variability in long tree-ring chronologies. Tree-Ring Res. **59**: 81–98.

Fritts, H.C., and Guiot, J. 1990. Methods of calibration, verification, and reconstruction. *In* Methods of dendrochronology. *Edited by* E.R. Cook and L.A. Kairiukstis. Kluwer Academic Publishers, Dordrecht, the Netherlands. pp. 163–217.

Guiot, J. 1993. The bootstrapped response function. Tree-Ring Bull. **51**: 39–41.

Hallett, R.A., Bailey, S.W., Horsley, S.B., and Long, R.P. 2006. Influence of nutrition and stress on sugar maple at a regional scale. Can. J. For. Res. **36**: 2235–2246. doi:10.1139/X06-120.

Hamburg, S.P., and Cogbill, C.V. 1988. Historical decline of red spruce populations and climatic warming. Nature (London), **331**: 428–431. doi:10.1038/331428a0.

Hogg, E.H., Hart, M., and Lieffers, V.J. 2002. White tree rings formed in trembling aspen saplings following experimental defoliation. Can. J. For. Res. **32**: 1929–1934. doi:10.1139/x02-114.

Horsley, S.B., Long, R.P., Bailey, S.W., Hallett, R.A., and Wargo, P.M. 2002. Health of eastern North American sugar maple forests and factors affecting decline. North. J. Appl. For. **19**: 34–44.

Houston, D.R., Parker, E.J., and Lonsdale, D. 1979. Beech bark disease: patterns of spread and development of the initiating agent *Cryptococcus fagisuga*. Can. J. For. Res. **9**: 336–344. doi:10.1139/x79-057.

Johnson, A.H., Cook, E.R., and Siccama, T.G. 1988. Climate and red spruce growth and decline in the northern Appalachians. Proc. Natl. Acad. Sci. U.S.A. **85**: 5369–5373. doi:10.1073/pnas.85.15.5369. PMID:16593962.

Johnson, A.H., Cook, E.R., Siccama, T.G., Battles, J.J., Mclaughlin, S.B., LeBlanc, D.C., and Wargo, P.M. 1995. Comment: Synchronic large-scale disturbances and red spruce growth decline. Can. J. For. Res. **25**: 851–858. doi:10.1139/x95-093.

LaMarche, V.C., Jr. 1974. Paleoclimatic inferences from long tree-ring records. Science (Washington, D.C.), **183**: 1043–1048. doi:10.1126/science.183.4129.1043. PMID:17738961.

Landis, R.M., and Peart, D.R. 2005. Early performance predicts canopy attainment across life histories in subalpine forest trees. Ecology, **86**: 63–72. doi:10.1890/03-0848.

Lazarus, B.E., Schaberg, P.G., DeHayes, D.H., and Hawley, G.J. 2004. Severe red spruce winter injury in 2003 creates unusual

ecological event in the northeastern United States. Can. J. For. Res. **34**: 1784–1788. doi:10.1139/x04-122.

Lazarus, B.E., Schaberg, P.G., Hawley, G.J., and DeHayes, D.H. 2006. Landscape-scale spatial patterns of winter injury to red spruce foliage in a year of heavy region-wide injury. Can. J. For. Res. **36**: 142–152. doi:10.1139/x05-236.

LeBlanc, D.C. 1992. Spatial and temporal variation in the prevalence of growth decline in red spruce populations of the northeastern United States. Can. J. For. Res. **22**: 1351–1363. doi:10.1139/x92-228.

Ledig, F.T., and Korbobo, D.R. 1983. Adaptation of sugar maple populations along altitudinal gradients — photosynthesis, respiration, and specific leaf weight. Am. J. Bot. **70**: 256–265. doi:10.2307/2443271.

Lorimer, C.G., and Frelich, L.E. 1989. A methodology for estimating canopy disturbance frequency and intensity in dense temperate forests. Can. J. For. Res. **19**: 651–663. doi:10.1139/x89-102.

Lorimer, C.G., Dahir, S.E., and Singer, M.T. 1999. Frequency of partial rings in *Acer saccharum* in relation to canopy position and growth rate. Plant Ecol. **143**: 189–202. doi:10.1023/A:1009847819158.

Lovett, G.M., and Mitchell, M.J. 2004. Sugar maple and nitrogen cycling in the forests of eastern North America. Front. Ecol. Environ, **2**: 81–88. doi:10.1890/1540-9295(2004)002[0081:SMANCI]2.0.CO;2.

Manion, P.D. 1991. Tree disease concepts. Prentice Hall, Englewood Cliffs, N.J.

McLauchlan, K.K., Craine, J.M., Oswald, W.W., Leavitt, P.R., and Likens, G.E. 2007. Changes in nitrogen cycling during the past century in a northern hardwood forest. Proc. Natl. Acad. Sci. U.S.A. **104**: 7466–7470. doi:10.1073/pnas.0701779104. PMID: 17446271.

Melvin, T.M. 2004. Historical growth rates and changing climatic sensitivity of boreal conifers. Ph.D. thesis. University of East Anglia, UK.

Myers, J.H. 1998. Synchrony in outbreaks of forest Lepidoptera in the Northern Hemisphere: a possible example of the Moran Effect. Ecology, **79**: 1111–1117.

Payette, S., Fortin, M.J., and Morneau, C. 1996. The recent sugar maple decline in southern Quebec: probable causes deduced from tree rings. Can. J. For. Res. **26**: 1069–1078. doi:10.1139/x26-118.

Reams, G.A., and Van Deusen, P.C. 1993. Synchronic large-scale disturbances and red spruce growth decline. Can. J. For. Res. **23**: 1361–1374. doi:10.1139/x93-173.

Schaberg, P.G. 2000. Winter photosynthesis in red spruce (*Picea rubens* Sarg.): limitations, potential benefits, and risks. Arct. Antarct. Alp. Res. **32**: 375–380. doi:10.2307/1552385.

Schaberg, P.G., DeHayes, D.H., and Hawley, G.J. 2001. Anthropogenic calcium depletion: a unique threat to forest ecosystem health? Ecosyst. Health, **7**: 214–228. doi:10.1046/j.1526-0992.2001.01046.x.

Schaberg, P.G., Tilley, J.W., Hawley, G.J., DeHayes, D.H., and Bailey, S.W. 2006. Associations of calcium and aluminum with the growth and health of sugar maple trees in Vermont. For. Ecol. Manage. **223**: 159–169. doi:10.1016/j.foreco.2005.10.067.

Siccama, T.G. 1974. Vegetation, soil, and climate on the Green Mountains of Vermont. Ecol. Monogr. **44**: 325–349. doi:10.2307/2937033.

St. Clair, S.B., Sharpe, W.E., and Lynch, J.P. 2008. Key interactions between nutrient limitation and climatic factors in temperate forests: a synthesis of the sugar maple literature. Can. J. For. Res. **38**: 401–414. doi:10.1139/X07-161.

Tardif, J., Brisson, J., and Bergeron, Y. 2001. Dendroclimatic analysis of *Acer saccharum*, *Fagus grandifolia*, and *Tsuga canadensis* from an old-growth forest, southwestern Quebec. Can. J. For. Res. **31**: 1491–1501. doi:10.1139/cjfr-31-9-1491.